PHYSICAL REVIEW E **96**, 020603(R) (2017)

Hydrodynamic interactions in dense active suspensions: From polar order to dynamical clusters

Natsuhiko Yoshinaga[1,2,3,*] and Tanniemola B. Liverpool[3,4,5,†]

[1]*WPI - Advanced Institute for Materials Research, Tohoku University, Sendai 980-8577, Japan*

[2]*MathAM-OIL, AIST, Sendai 980-8577, Japan*

[3]*The Kavli Institute for Theoretical Physics, University of California, Santa Barbara, California 93106, USA*

[4]*School of Mathematics, University of Bristol, Bristol BS8 1TW, United Kingdom*

[5]*BrisSynBio, Tyndall Avenue, Bristol BS8 1TQ, United Kingdom*

(Received 4 July 2016; revised manuscript received 26 March 2017; published 29 August 2017)

We study the role of hydrodynamic interactions in the collective behavior of collections of microscopic active particles suspended in a fluid. We introduce a calculational framework that allows us to separate the different contributions to their collective dynamics from hydrodynamic interactions on different length scales. Hence we are able to systematically show that lubrication forces when the particles are very close to each other play as important a role as long-range hydrodynamic interactions in determining their many-body behavior. We find that motility-induced phase separation is suppressed by near-field interactions, leading to open gel-like clusters rather than dense clusters. Interestingly, we find a globally polar ordered phase appears for neutral swimmers with no force dipole that is enhanced by near-field lubrication forces in which the collision process rather than long-range interaction dominates the alignment mechanism.

DOI: 10.1103/PhysRevE.96.020603

Active materials are condensed matter systems self-driven out of equilibrium by components that convert stored energy into movement. They have generated much interest recently, both as inspirations for new smart materials and as a framework to understand aspects of cell motility [1–3]. They are characterized by interesting nonequilibrium collective phenomena, such as swirling, alignment, pattern formation, dynamic cluster formation, and phase separation [4–8]. Theoretical descriptions of active systems range from continuum models [1,9] to discrete collections of self-propelled active particles [4]. An influential classification of self-propelled active particle systems has been to group them into *dry* and *wet* systems [1]. Dry systems do not have momentum conserving dynamics [e.g., Vicsek models [4,9] and active Brownian particle (ABP) models interacting via soft *repulsive* potentials [10–12]], while wet systems conserve momentum via a coupling to a fluid (e.g., squirmers driven by surface deformations [13–15] and Janus particles driven by surface chemical reactions [16]) leading to hydrodynamic interactions between active particles. Dealing with hydrodynamics leads to significant technical hurdles, as the motion of a self-propelled swimmer is affected by other particles due to both fluid flow and pressure, and even the two-body interaction between spherical squirmers in close proximity (near field) is nontrivial, requiring sophisticated numerical analyses [17–23]. Therefore, converting this into an understanding of collective behavior remains a significant challenge [24]. Because numerical simulations with hydrodynamics require significantly more computational power, studies of these systems have relatively few particles or low resolution of fluid flow [25–28]. Hence, far-field approximations (swimmers as point multipoles) [29] are often used to account for hydrodynamic interactions [30]. This clearly breaks down when the swimmers are close to one another, limiting the validity of such studies to very dilute suspensions.

The appearance of dynamical clusters [11,31] in recent experiments on active particles has generated much interest. This has been linked to a clustered state observed in two-dimensional (2D) ABP systems called motility-induced phase separation (MIPS) [10–12,32] and for squirmers confined between walls [26,33]. A major difference, however, is finite-size clusters in experiments [7,11,31] compared to the infinite cluster formed in MIPS. In addition, recent simulations have shown that clusters are absent in 2D squirmer suspensions and in a 2D squirmer monolayer embedded in a three-dimensional (3D) fluid [27,34]. While attractive interactions can lead to clustering [35–37], here we study swimmers with purely repulsive interactions to see the role of hydrodynamics in active cluster formation.

It is accepted from continuum arguments that the polar state is generically unstable for wet active systems [1–3], however, recent simulations of wet active particles have raised the interesting possibility of other continuum limits in these systems. A polar state has been observed for neutral squirmers with no force dipole with 3D hydrodynamics, but 2D motion [19] and in 3D [38–40]. It has been suggested [19] that near-field effects *enhance* the polar state, although there are hints that far-field effects also play a role [19]. These results are limited by relatively few particles, so it is natural to ask if the polar state is present in the thermodynamic limit.

In this Rapid Communication, we systematically construct equations of motion for wet active particles, namely, the dynamics of their position and orientation. One of our aims is to provide a computationally tractable model of comparable complexity to ABP which takes account of hydrodynamic interactions of particles in close proximity [17,41]. Using it, we study a suspension of force-free and torque-free repulsive *spherical* squirmers and obtain the phase behavior summarized in Fig. 2 as a function of density ρ_0. In studying the phase behavior, we have emphasized the dependences on the sign of the force dipole (v_2) and contrasted them to neutral swimmers

*yoshinaga@tohoku.ac.jp

†t.liverpool@bristol.ac.uk

with a force quadrupole and no force dipole ($v_2 = 0$). We find significant differences between the hydrodynamic interactions with and without near-field effects. The phase behaviors of neutral swimmers ($v_2 = 0$) with only *far-field* interactions are similar to those of ABPs since there are no collision-induced reorientations. Upon including near-field effects, we obtain phase diagrams characterized by, at low densities, a disordered "gas" state, and at higher densities, the emergence of stable "static clusters" except for neutral swimmers [42] which spontaneously develop polar order. Dense static clusters, present in far-field only systems, are suppressed by the near-field interactions, leading to open gel-like clusters. In between the gas and static cluster are phases of "dynamic clusters" of finite size that exchange particles with the bulk. While the boundaries between different clustered phases are qualitative and threshold dependent, the boundaries between the polar state and other states have all the features associated with a phase transition.

Each particle (squirmer) is characterized by its position and orientation $(\mathbf{r}^{(i)}, \mathbf{p}^{(i)})$ with dynamics given by

$$\dot{\mathbf{r}}^{(i)} = \mathbf{u}^{(i)}, \quad \dot{\mathbf{p}}^{(i)} = \boldsymbol{\omega}^{(i)} \times \mathbf{p}^{(i)}, \quad |\mathbf{p}^{(i)}| = 1. \tag{1}$$

The translational and angular velocities of each particle, $\mathbf{u}^{(i)}$ and $\boldsymbol{\omega}^{(i)}$, respectively, are obtained by solving for the fluid mediated interaction between all pairs of particles The fluid is taken as incompressible with vanishing Re,

$$\eta \nabla^2 \mathbf{v} - \nabla p = \mathbf{0}, \quad \nabla \cdot \mathbf{v} = 0, \tag{2}$$

where η is the viscosity, $\mathbf{v}(\mathbf{r})$ is the velocity, and $p(\mathbf{r})$ the pressure. The boundary condition on the swimmer surface is a sum of rigid translational, $\mathbf{u}$, and rotational, $\boldsymbol{\omega}$, motion and an active slip flow, $\mathbf{v}_s$, driving self-propulsion,

$$\mathbf{v}|_{\mathbf{r}=\mathbf{R}} = \mathbf{u} + \boldsymbol{\omega} \times \mathbf{R} + \mathbf{v}_s, \tag{3}$$

$$\mathbf{v}_s = \sum_{l=1}^{\infty} \sum_{m=-l}^{l} [v_{lm} \boldsymbol{\Psi}_{lm}(\theta,\varphi) + w_{lm} \boldsymbol{\Phi}_{lm}(\theta,\varphi)], \tag{4}$$

for a swimmer with the center at the origin. The fluid velocity vanishes at infinity, $\mathbf{v}|_{r\to\infty} = \mathbf{0}$, with θ the polar angle with the z axis and azimuthal φ with the x axis on the xy plane. The slip velocity $\mathbf{v}_s$ can be very efficiently expanded in the tangential vector spherical harmonics, $\boldsymbol{\Psi}_{lm}$ and $\boldsymbol{\Phi}_{lm}$ [43,44]. The second term in (4) represents rotational slip around the swimmer axis associated with spinning motion which we neglect in the following, and from now on set $w_{lm} = 0$. The swimmer axis $\mathbf{p}$ is a unit vector (see Fig. 1).

For uniaxial particles, v_{lm} is a function of a magnitude v_l and the swimmer orientation $\mathbf{p}$ [44]. An isolated squirmer moves with the velocity $\mathbf{u}_0^{(i)} = u_0 \mathbf{p}^{(i)}$ with $u_0 = -\frac{2}{3}\sqrt{\frac{3}{4\pi}} v_1$.

Given two squirmers, separated by $\mathbf{r}_{ij}$, the flow field generated by one will affect the other and hence lead to modification of the self-propulsion velocities. We split the problem into two parts, a force and torque, acting on the sphere with, first, slip boundary conditions without translational and rotational motion ($\mathbf{F}^{(a)}$, $\mathbf{T}^{(a)}$, the active problem), and second, with the nonslip boundary conditions undergoing rigid-body motion $\mathbf{u}^{(i)}$ and $\boldsymbol{\omega}^{(i)}$ ($\mathbf{F}^{(p)}$, $\mathbf{T}^{(p)}$, the passive problem) [44]. The force-free and torque-free conditions imply $\mathbf{F}^{(a)} + \mathbf{F}^{(p)} = \mathbf{0}$ and $\mathbf{T}^{(a)} + \mathbf{T}^{(p)} = \mathbf{0}$ which determine $\mathbf{u}^{(i)}$ and $\boldsymbol{\omega}^{(i)}$. The problems can be solved exactly for pairs of particles in two asymptotic limits: (1) when their separation, $h_{ij} = r_{ij} - 2R$, $r_{ij} = |\mathbf{r}_{ij}|$, is much less than their radius (near field) and (2) when their separation is much greater than their radius (far field). For arbitrary separations between particles, we interpolate between the two limits, far field and near field, using the tanh function. There is a long history of calculation of the passive problem [45,46]. Here, we compute the active problem for both far field and near field in the general setting. Previous near-field active results have been obtained only for axisymmetric surface flow fields [17]. It should be noted that to obtain the velocity and angular velocity for collections of swimmers, one must solve the active and passive problems for *all* possible relative orientations [23].

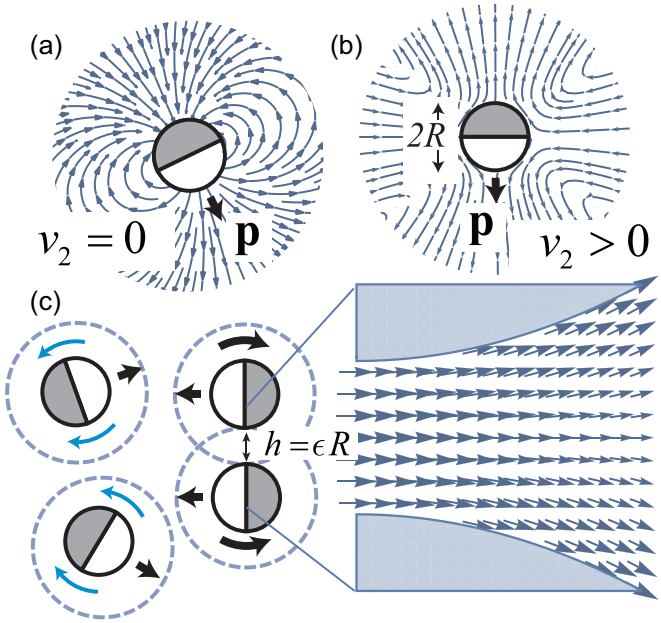

FIG. 1. Schematic interaction between swimmers. Each particle creates a leading-order (a) quadrupolar or (b) dipolar flow. (c) When two particles are very close to each other, lubrication flow dominates the interactions.

For a pair of squirmers (labeled i, j) with arbitrary positions (and orientation), we define a spherical coordinate system: relative separations $r_{ij} = |\mathbf{r}_{ij}|$, polar angles θ_{ij}, and azimuthal angles φ_{ij}. Using it, a general form for the velocities valid in both far- and near-field limits is

$$\mathbf{u}^{(i)} = \mathbf{u}_0^{(i)} \lambda^{(i)} + \sum_{j\neq i,l,m} \left[u_{lm,\parallel}^{(ji)} \mathbf{Y}_{lm}^{(ji)} + u_{lm,\perp}^{(ji)} \boldsymbol{\Psi}_{lm}^{(ji)} \right], \tag{5}$$

$$\boldsymbol{\omega}^{(i)} = \sum_{j\neq i,l,m} \omega_{lm}^{(ji)} \boldsymbol{\Phi}_{lm}^{(ji)}, \tag{6}$$

where $\boldsymbol{\Psi}_{lm}^{(ji)} = \boldsymbol{\Psi}_{lm}(\theta_{ji},\varphi_{ji})$, $\boldsymbol{\Phi}_{lm}^{(ji)} = \boldsymbol{\Phi}_{lm}(\theta_{ji},\varphi_{ji})$, $\mathbf{Y}_{lm}^{(ji)} = \mathbf{Y}_{lm}(\theta_{ji},\varphi_{ji})$, with the $\mathbf{Y}_{lm}(\theta,\varphi)$ the normal vector spherical harmonics. For the far field, $u_{1,m,\parallel}^{(ji)} \sim u_{1,m,\perp}^{(ji)} \sim r_{ij}^{-3}$ (quadrupole), $u_{2,m,\parallel}^{(ji)} \sim r_{ij}^{-2}$, and $\omega_{2,m}^{(ji)} \sim r_{ij}^{-3}$ (dipole). For the near field, $u_{lm,\parallel}^{(ji)} \sim \epsilon \log \epsilon$ and $u_{lm,\perp}^{(ji)} \sim \omega_{lm}^{(ji)} \sim \epsilon^0$ with $\epsilon = (r_{ij} - 2R)/R$ [44]. $\lambda^{(i)} = 1$ when the ith particle is away

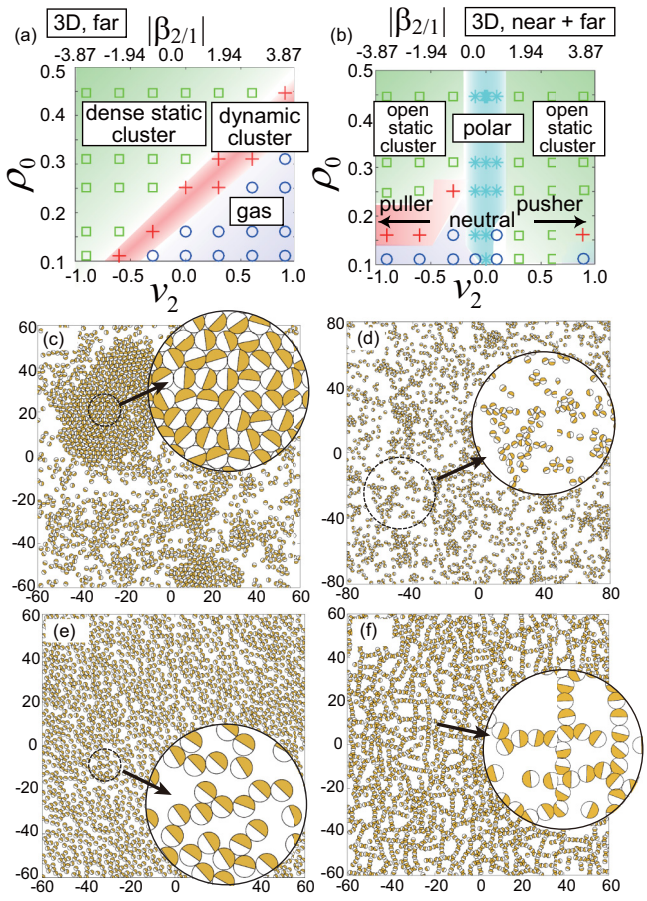

FIG. 2. The state diagram of squirmers with density (ρ_0) and dipolar strength (v_2) with (a) far-field hydrodynamic interactions and (b) both far field and near field with $N = 2048$ particles. Snapshots of (c) the static dense cluster state for a far-field-only system ($\phi = 0.447$, $v_2 = 0$), (d) the dynamic cluster state ($\phi = 0.251$, $v_2 = 0$), (e) the polar state ($\phi = 0.447$, $v_2 = 0$), and (f) the static open cluster state for a near+far system ($\phi = 0.447$, $v_2 = 0.9$).

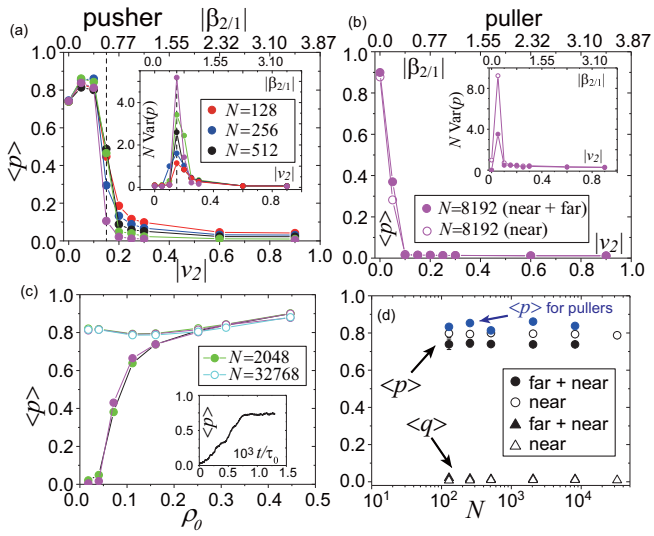

FIG. 3. (a), (b) The mean polarity as a function of the dipolar slip flow v_2 on a squirmer at $\rho_0 = 0.16$ ($\xi = 4.43$). The corresponding values of the squirmer index $\beta_{2/1}$ are shown at the upper axis. The polar order $\langle p \rangle$ for pushers (a) and pullers (b). The insets in (a) and (b) show the variance of the polar order. Solid circles indicate the system with the near and far fields whereas open circles indicate the near-field-only system. (c) The mean polarity $\langle p \rangle$ for neutral swimmers $v_2 = 0$ vs density ρ_0 (inset: time evolution of $\langle p \rangle$). The solid (open) symbols correspond to the simulations with (without) the far-field interaction. Both include the near-field interaction. (d) The system size dependence of the mean polar order $\langle p \rangle$ and the mean cluster ratio $\langle q \rangle$ at $\rho_0 = 0.16$ ($\xi = 4.43$) of the neutral swimmer $v_2 = 0$ (black). Both the simulations with far- and near-field interactions and only near-field interactions are shown. The results of the simulations with far- and near-field interactions for weak pushers $v_2 = 0.05$ are also shown in blue. The legends are shared by all the figures.

from the near-field region of any other particles and $\lambda^{(i)} = 0$ otherwise.

Equations (1), (6), and (5) form a closed complete dynamical system. Using them, we performed numerical simulations of N identical particles of radius R with periodic boundary conditions. Figure 2 shows various state points of this model as a function of the density $\rho_0 = \pi R^2 N/L^2$ and the force dipole strength v_2. Most have $N = 2048$ unless otherwise specified. Defining the average distance between two particles, $\xi = R\sqrt{\pi/\rho_0}$, we vary ξ from $\xi \simeq 2.65$ to $\xi \simeq 5.30$. We set $v_1 = 1$ for all swimmers and thus $u_0 \simeq 0.32$.

The size of a particle is chosen to be of unit length, thus we set $R = 1$. The time scale is normalized by the time for an isolated squirmer to move a half of its body length, that is, $\tau_0 = R/u_0$. There is a time scale associated with collisions, $\tau_m = \xi/u_0$. We vary the time scale from $\tau_m \simeq 8$ to $\tau_m \simeq 17$. We consider motion restricted to 2D *but* interacting via 3D hydrodynamic interactions. We neglect the modes with $l \geqslant 3$. We note that for 3D hydrodynamics projected onto 2D, pushers and pullers are not identical; the interaction at the front and the back is stronger than that at the side. As a result, pullers, on average, attract nearby objects. We find a global phase separation of active particles with repulsive interactions, i.e., MIPS, is suppressed by near-field hydrodynamics and we find instead networks of open clusters for a large range of intermediate densities. We see a gel-like extended state at high enough densities.

Most surprisingly we find that for neutral (quadrupolar) squirmers and squirmers with small dipoles, $|v_2| \ll 1$, the swimmers self-organize into a polar state with aligned orientations and swimming directions. This polar order vanishes at low density. Screening far-field interactions [47] leads to polar order at lower densities [see Fig. 3(c)]. As $|v_2|$ is increased, polar order vanishes. For example, for pushers ($v_2 > 0$), polar order disappears at $v_2^* \simeq 0.15$ ($\beta_{2/1} \simeq 0.58$) in Fig. 3(a). The loss of polar order is accompanied by a divergence of fluctuations of the polarity as shown in Fig. 3(a). The position of the phase boundary is not symmetric about $v_2 = 0$, i.e., different $|v_2^*|$ for pushers and pullers [see Fig. 3(b)].

We check the stability of polar order to fluctuations by adding Gaussian white noise of amplitude σ to the rotation in Eq. (1). At a fixed density ρ_0 we find a transition from a gas to a polar state at a critical value of $\sigma_c > 0$.

Polar order remains as we increase the system size. In Fig. 3(d), polar order is shown as a function of the number

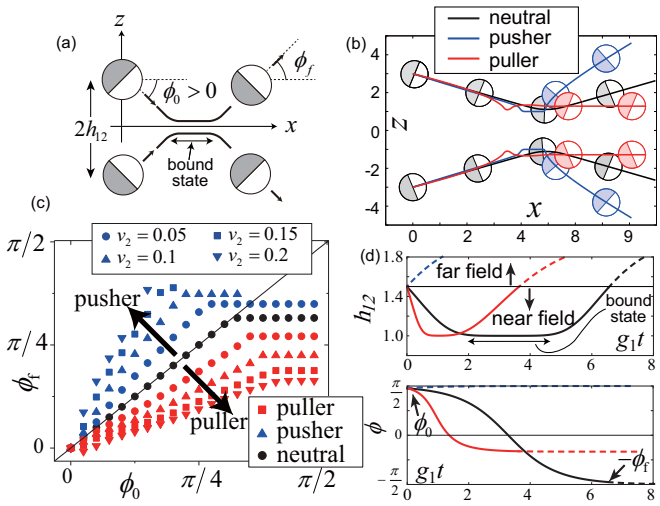

FIG. 4. (a) Schematics of two-body collisions. (b) Typical trajectories for neutral, pusher, and puller swimmers are shown. (c) The incidence ϕ_0 and reflection ϕ_f angles for symmetric collisions for neutral swimmers ($v_2 = 0$) and small nonzero values of v_2: pushers ($v_2 > 0$) and pullers ($v_2 < 0$). The solid line shows $\phi_0 = \phi_f$. Only the range of $0 \leqslant \phi_0$, $\phi_f \leqslant \pi/2$ is shown. (d) The dynamics of the separation $h_{12}(t)$ and the angle $\phi(t)$ in the near-field region for $g_2/g_1 = 1$. Here, $g_1 \sim u_0/R$ and $g_2 \sim v_2/R$ [44]. The time scale is normalized by g_1^{-1}. Motion outside the near-field region is indicated by dashed lines. The legends are shared by all the figures.

of particles N up to $N = 8192$ for the near+far-field system and $N = 32\,768$ for the near-field-only system. Therefore, we conclude that the system is asymptotically in a state with macroscopic global polar order. However, we are not able to exclude the possibility that it disappears at much larger system sizes, even though we cannot identify an obvious physical mechanism by which that might happen. The mean cluster ratio $\langle q \rangle$, the fraction of swimmers in large clusters, is nearly zero throughout the polar phase [see Fig. 3(d)], indicating clusters are not associated with polar order.

It is evident from the simulations that collisions between the particles are key in the development of polar order. Hence, we explore a two-body collision in detail [see Fig. 4(a) and Ref. [44]]. Figure 4(b) shows some trajectories of two "colliding" squirmers.

For the far-field only system, any transient alignment of pairs of squirmers is unstable to rotational fluctuations arising from collisions with other particles and no polar order is developed. Including the near-field (lubrication) interaction, however, leads to reorientation, while in the transient bound [Fig. 4(a)] states occurring during collisions, as shown in Fig. 4(d). For small incident angles ($|\phi_0| \lesssim \pi/4$), collisions are symmetric, i.e., the reflection angle (ϕ_f) equals ϕ_0 but for as $|\phi_0|$ increases, $|\phi_f|$ stops increasing and tends to a finite (*saturation*) angle $\lesssim \pi/4$. This asymmetry between incident and reflection angles means [$\langle|\phi_f|\rangle < \langle|\phi_0|\rangle$, see Fig. 4(c)] and leads eventually to alignment. This effect is most pronounced for neutral swimmers ($v_2 = 0$); while similar behavior is seen for pushers and pullers, shorter residence times for pullers [Fig. 4(d)] and larger reflection angles for pushers [Fig. 4(c)] eventually destroy the polar state for both of them as $|v_2|$ becomes large. The saturation angle in Fig. 4(c) is due to direct contacts between squirmers (repulsive forces from the interaction potential). This reorientation depends weakly on the contact interaction; big changes in the interaction potential lead only to slight shifts of the saturation angles. Hence the collective behavior and phase boundaries are independent of the choice of potential [44].

While we only considered pairwise interactions, combining many of them results in many-body effects which become relevant for a nondilute suspension. In fact, for a dense suspension, the dynamics is dominated by the lubrication interaction between swimmers, which is well approximated by a sum of two-body interactions. We note, in particular, that $\langle p \rangle$ is independent of N even for $v_2 \neq 0$ (i.e., weak pushers) as shown in Fig. 3(d). To understand how these many-body effects give rise to collective behavior, we have carried out numerical simulations of a minimal model, in which the only nonzero interactions are rotational near field: $\omega_{lm}^{(ij)} \sim \epsilon^0$ [44] plus noise. It has two key ingredients: short-range orientational interactions and short-range repulsive interactions. We are able to reproduce the same polar-disorder phase transition by increasing the noise amplitude. We conclude that the detailed forms of the hydrodynamic interactions are not essential for the development of polar order. In contrast to the Vicsek model, here the lack of an alignment rule means excluded volume interactions are required to generate polar order. We observed density bands near the critical point of the order-disorder transition induced by noise for neutral swimmers and the minimal model mentioned above [48]. While this is reminiscent of variants of the Vicsek model, we note that here the polar order is destabilized not only by noise but also by the dipolar interactions.

The existence of polar order is fundamentally surprising because of the apparent contradiction with the well-accepted generic instability of polar and nematic order of wet active matter [1,49]. To understand this we construct a two-fluid model for the system which allows a macroscopic relative flux between swimmers and suspending fluid at small wave numbers k: the suspending fluid (volume fraction $1 - \phi$) with velocity $\mathbf{v}(\mathbf{r},t)$ and the active particle (squirmer) "phase" (volume fraction ϕ) with local displacement variable $\mathbf{u}(\mathbf{r},t)$ due to squirmer density variations. Finally, we identify a *local* polar order parameter $\mathbf{p}(\mathbf{r},t)$. Our analysis highlights collisions of the swimmers as essential for the formation of polar order. An isolated squirmer swims with velocity $u_0\mathbf{p}$ relative to the background fluid. The fluid obeys the Stokes equation with a force density $\mathbf{f}^c \sim O(\rho_a^2)$ due to collisions between squirmers and an active stress $\sigma_{ij}^a = \zeta p_i p_j$, where $\zeta \propto v_2$ and $\rho_a = \phi\rho$ is the average density of active particles.

Replacing $\mathbf{f}^c$ by $\chi(\dot{\mathbf{u}} - \mathbf{v} - u_0\mathbf{p})$, and linearizing $\mathbf{p},\mathbf{v}$ about the homogeneous polar state, $\mathbf{p} = \mathbf{p}_0$ and $\mathbf{v}_0 = \dot{\mathbf{u}}_0 - u_0\mathbf{p}_0$,

$$\mathbf{0} = \eta\nabla^2\delta\mathbf{v} + \chi\delta\mathbf{v} - \nabla P + \nabla\cdot\boldsymbol{\sigma}^a, \quad \nabla\cdot\delta\mathbf{v} = 0, \quad (7)$$

$$\partial_t\delta\mathbf{p} = -u_0\mathbf{p}_0\cdot\nabla\delta\mathbf{p} + \delta\boldsymbol{\omega}\cdot\mathbf{p}_0 + \gamma\delta\mathbf{e}\cdot\mathbf{p}_0 + K\nabla^2\delta\mathbf{p}, \quad (8)$$

where $\omega_{ij} = \frac{1}{2}(\partial_i v_j - \partial_j v_i)$, $e_{ij} = \frac{1}{2}(\partial_i v_j + \partial_j v_i)$, and K is the Frank elastic constant in the one constant approximation. A finite screening length $\xi \sim \sqrt{\eta/\chi}$ weakens the generic

instability from long wavelengths to finite wavelengths and stabilizes the polar state on long length scales. Hence a comparison between the screening length ξ and the active length scale $\sqrt{K/|\zeta|}$ [50] allows us to determine the onset of polar order for $|\zeta| < \zeta_c = K/\xi^2$, i.e., for swimmers that are close to neutral. We recover the generic instability as $\phi \to 0$.

We emphasize that the computational expense of including hydrodynamics in the simulations of collective behavior of active matter requires trade-offs where accuracy is sacrificed. Navier-Stokes (NS) solvers such as the lattice Boltzmann compromise on the resolution of the velocity field and hence do not accurately describe fluid flow when the active particles are very close to each other. Here, we have developed another scheme whose strengths are exactly where NS solvers are weak, for active particles in close proximity. It is also very accurate when the particles are well separated. Where it is less accurate, however, is at intermediate separations. Its other great advantage is the ease with which we can study systems with many more particles. Another nice feature is the ability to switch off different contributions to the motion to identify the dominant mechanisms behind the macroscopic phenomena observed. Using it we have studied the collective behavior of large numbers of spherical active particles and confirmed and clarified the phenomena observed in smaller simulations. Dense cluster formation is suppressed and we show that it is replaced by open gel-like aggregates at higher densities and, most surprisingly, a polar ordered phase is stabilized by hydrodynamic lubrication interactions. We have also provided analytic continuum arguments explaining how such a state can be realized. In addition to the work presented here, we have studied purely 2D systems (2D with 2D interactions) and 3D systems (3D with 3D interactions), and obtained similar results, but at higher densities [48].

The authors are grateful to S. Fielding, T. Ishikawa, and R. Golestanian for helpful discussions. N.Y. acknowledges the support by Japan Society for the Promotion of Science (JSPS) KAKENHI Grants No. JP26800219, No. JP17K05605, and No. JP16H00793. N.Y. also acknowledges the support by JSPS A3 Foresight Program. T.B.L. is supported by BrisSynBio, a Biotechnology and Biological Sciences Research Council/Engineering and Physical Sciences Research Council (BBSRC/EPSRC) Advanced Synthetic Biology Research Center (Grant No. BB/L01386X/1). We would like to thank the Isaac Newton Institute for Mathematical Sciences, Cambridge, for support and hospitality during the program "The Mathematics of Liquid Crystals" and "Dynamics of active suspensions, gels, cells and tissues," where work on this article was started.

[1] M. C. Marchetti, J. F. Joanny, S. Ramaswamy, T. B. Liverpool, J. Prost, M. Rao, and R. Aditi Simha, Hydrodynamics of soft active matter, Rev. Mod. Phys. **85**, 1143 (2013).

[2] J. Toner, Y. Tu, and S. Ramaswamy, Hydrodynamics and phases of flocks, Ann. Phys. **318**, 170 (2005).

[3] S. Ramaswamy, The mechanics and statistics of active matter, Annu. Rev. Condens. Matter Phys. **1**, 323 (2010).

[4] T. Vicsek, A. Czirók, E. Ben-Jacob, I. Cohen, and O. Shochet, Novel Type of Phase Transition in a System of Self-Driven Particles, Phys. Rev. Lett. **75**, 1226 (1995).

[5] H. H. Wensink, J. Dunkel, S. Heidenreich, K. Drescher, R. E. Goldstein, H. Löwen, and J. M. Yeomans, Meso-scale turbulence in living fluids, Proc. Natl. Acad. Sci. USA **109**, 14308 (2012).

[6] M. E. Cates, Diffusive transport without detailed balance in motile bacteria: Does microbiology need statistical physics?, Rep. Prog. Phys. **75**, 042601 (2012).

[7] J. Palacci, S. Sacanna, A. P. Steinberg, D. J. Pine, and P. M. Chaikin, Living crystals of light-activated colloidal surfers, Science **339**, 936 (2013).

[8] A. Bricard, J.-B. Caussin, N. Desreumaux, O. Dauchot, and D. Bartolo, Emergence of macroscopic directed motion in populations of motile colloids, Nature (London) **503**, 95 (2013).

[9] E. Bertin, H. Chaté, F. Ginelli, S. Mishra, A. Peshkov, and S. Ramaswamy, Mesoscopic theory for fluctuating active nematics, New J. Phys. **15**, 085032 (2013).

[10] Y. Fily and M. C. Marchetti, Athermal Phase Separation of Self-Propelled Particles with No Alignment, Phys. Rev. Lett. **108**, 235702 (2012).

[11] I. Buttinoni, J. Bialké, F. Kümmel, H. Löwen, C. Bechinger, and T. Speck, Dynamical Clustering and Phase Separation in Suspensions of Self-Propelled Colloidal Particles, Phys. Rev. Lett. **110**, 238301 (2013).

[12] G. S. Redner, M. F. Hagan, and A. Baskaran, Structure and Dynamics of a Phase-Separating Active Colloidal Fluid, Phys. Rev. Lett. **110**, 055701 (2013).

[13] M. J. Lighthill, On the squirming motion of nearly spherical deformable bodies through liquids at very small Reynolds numbers, Commun. Pure Appl. Math. **5**, 109 (1952).

[14] J. R. Blake, Self propulsion due to oscillations on the surface of a cylinder at low reynolds number, Bull. Aust. Math. Soc. **5**, 255 (1971).

[15] O. S. Pak and E. Lauga, Generalized squirming motion of a sphere, J. Eng. Math. **88**, 1 (2014).

[16] R. Golestanian, T. B. Liverpool, and A. Ajdari, Propulsion of a Molecular Machine by Asymmetric Distribution of Reaction Products, Phys. Rev. Lett. **94**, 220801 (2005).

[17] T. Ishikawa, M. P. Simmonds, and T. J. Pedley, Hydrodynamic interaction of two swimming model micro-organisms, J. Fluid Mech. **568**, 119 (2006).

[18] I. Llopis and I. Pagonabarraga, Dynamic regimes of hydrodynamically coupled self-propelling particles, Europhys. Lett. **75**, 999 (2006).

[19] T. Ishikawa, J. T. Locsei, and T. J. Pedley, Development of coherent structures in concentrated suspensions of swimming model micro-organisms, J. Fluid Mech. **615**, 401 (2008).

[20] K. Ishimoto and E. A. Gaffney, Squirmer dynamics near a boundary, Phys. Rev. E **88**, 062702 (2013).

[21] G.-J. Li and A. M. Ardekani, Hydrodynamic interaction of microswimmers near a wall, Phys. Rev. E **90**, 013010 (2014).

[22] N. Sharifi-Mood, A. Mozaffari, and U. Córdova-Figueroa, Pair interaction of catalytically active colloids: From assembly to escape, J. Fluid Mech. **798**, 910 (2016).

[23] D. Papavassiliou and G. P. Alexander, Exact solutions for hydrodynamic interactions of two squirming spheres, J. Fluid Mech. **813**, 618 (2017).

[24] P. J. Mucha, S.-Y. Tee, D. A. Weitz, B. I. Shraiman, and M. P. Brenner, A model for velocity fluctuations in sedimentation, J. Fluid Mech. **501**, 71 (2004).

[25] J. J. Molina, Y. Nakayama, and R. Yamamoto, Hydrodynamic interactions of self-propelled swimmers, Soft Matter **9**, 4923 (2013).

[26] A. Zöttl and H. Stark, Hydrodynamics Determines Collective Motion and Phase Behavior of Active Colloids in Quasi-Two-Dimensional Confinement, Phys. Rev. Lett. **112**, 118101 (2014).

[27] R. Matas-Navarro, R. Golestanian, T. B. Liverpool, and S. M. Fielding, Hydrodynamic suppression of phase separation in active suspensions, Phys. Rev. E **90**, 032304 (2014).

[28] J.-B. Delfau, J. Molina, and M. Sano, Collective behavior of strongly confined suspensions of squirmers, Europhys. Lett. **114**, 24001 (2016).

[29] S. E. Spagnolie and E. Lauga, Hydrodynamics of self-propulsion near a boundary: Predictions and accuracy of far-field approximations, J. Fluid Mech. **700**, 105 (2012).

[30] D. Saintillan and M. J. Shelley, Theory of active suspensions, in *Complex Fluids in Biological Systems* (Springer, Berlin, 2015), pp. 319–355.

[31] I. Theurkauff, C. Cottin-Bizonne, J. Palacci, C. Ybert, and L. Bocquet, Dynamic Clustering in Active Colloidal Suspensions with Chemical Signaling, Phys. Rev. Lett. **108**, 268303 (2012).

[32] F. Peruani, A. Deutsch, and M. Bär, Nonequilibrium clustering of self-propelled rods, Phys. Rev. E **74**, 030904 (2006).

[33] J. Blaschke, M. Maurer, K. Menon, A. Zöttl, and H. Stark, Phase separation and coexistence of hydrodynamically interacting microswimmers, Soft Matter **12**, 9821 (2016).

[34] P. G. Saffman and M. Delbrück, Brownian motion in biological membranes, Proc. Natl. Acad. Sci. USA **72**, 3111 (1975).

[35] S. Saha, R. Golestanian, and S. Ramaswamy, Clusters, asters, and collective oscillations in chemotactic colloids, Phys. Rev. E **89**, 062316 (2014).

[36] R. M. Navarro and S. M. Fielding, Clustering and phase behavior of attractive active particles with hydrodynamics, Soft Matter **11**, 7525 (2015).

[37] F. Alarcón, C. Valeriani, and I. Pagonabarraga, Morphology of clusters of attractive dry and wet self-propelled spherical particle suspensions, Soft Matter **13**, 814 (2017).

[38] A. A. Evans, T. Ishikawa, T. Yamaguchi, and E. Lauga, Orientational order in concentrated suspensions of spherical microswimmers, Phys. Fluids **23**, 111702 (2011).

[39] F. Alarcón and I. Pagonabarraga, Spontaneous aggregation and global polar ordering in squirmer suspensions, J. Mol. Liq. **185**, 56 (2013).

[40] J. J. Molina, N. Oyama, and R. Yamamoto, A binary collision route for purely hydrodynamic orientational ordering of microswimmers, arXiv:1606.03839.

[41] J. W. Swan, J. F. Brady, R. S. Moore, and ChE 174, Modeling hydrodynamic self-propulsion with Stokesian dynamics. or teaching Stokesian dynamics to swim, Phys. Fluids **23**, 071901 (2011).

[42] See Ref. [44] for the definitions of the polar order and the clusters.

[43] E. L. Hill, The theory of vector spherical harmonics, Am. J. Phys. **22**, 211 (1954).

[44] See Supplemental Material at http://link.aps.org/supplemental/10.1103/PhysRevE.96.020603 for details of the formula and the numerical simulations.

[45] D. J. Jeffrey and Y. Onishi, Calculation of the resistance and mobility functions for two unequal rigid spheres in low-Reynolds-number flow, J. Fluid Mech. **139**, 261 (1984).

[46] S. Kim and S. J. Karrila, *Microhydrodynamics* (Butterworth-Heinemann, New York, 1991).

[47] R. C. Ball and J. R. Melrose, A simulation technique for many spheres in quasi-static motion under frame-invariant pair drag and Brownian forces, Physica A **247**, 444 (1997).

[48] N. Yoshinaga and T. B. Liverpool (unpublished).

[49] R. Aditi Simha and S. Ramaswamy, Hydrodynamic Fluctuations and Instabilities in Ordered Suspensions of Self-Propelled Particles, Phys. Rev. Lett. **89**, 058101 (2002).

[50] R. Voituriez, J. F. Joanny, and J. Prost, Spontaneous flow transition in active polar gels, Europhys. Lett. **70**, 404 (2005).